

Can substructure in the Galactic Halo explain the ATIC and PAMELA results?

Pascal J. Elahi¹, Lawrence M. Widrow¹, Robert J. Thacker²

¹*Department of Physics, Engineering Physics & Astronomy, Queen's University, Kingston, Ontario, Canada; pelahi@astro.queensu.ca, widrow@astro.queensu.ca*

²*Department of Astronomy & Physics, Saint Mary's University, Halifax, Nova Scotia, Canada; thacker@ap.stmarys.ca*

Recently, ATIC and PAMELA measured an anomalously large flux of leptonic cosmic rays which may arise from dark matter self-annihilation. While the annihilation signal predicted for a smooth halo is $10^2 - 10^3$ times smaller than the measured excess, the signal can be boosted by the presence of subhalos. We investigate the feasibility of large boost factors using a new Monte Carlo calculation technique that is constrained by previous simulation work on halo substructure. The model accounts for the observed decrease in the amount of substructure with decreasing halo mass and the scatter in halo structural parameters such as the density concentration parameter. Our results suggest that boost factors of $\sim 10^2$ are ruled out at $\gtrsim 14\sigma$. We conclude that substructure alone, at least with commonly assumed annihilation cross-sections, cannot explain the anomalous flux measured by ATIC and PAMELA.

PACS numbers: 95.35.+d, 95.85.Ry, 95.85.Pw

Recent measurements by ATIC [1] and PAMELA [2] offer the tantalizing prospect that dark matter has been discovered, albeit indirectly. Both experiments have reported an anomalously large flux in leptonic cosmic rays at energies above 10 GeV. Dark matter candidates, such as WIMPs (Weakly Interacting Massive Particles which arise in theories of supersymmetry) or Kaluza-Klein particles, can annihilate and produce cosmic rays [3]. The excess flux might comprise secondary particles from annihilation events in the Galactic halo, a possibility that is now attracting considerable attention.

Though the observed anomalous flux is 100-1000 times larger than the flux predicted from a smooth Milky Way halo with a standard thermal WIMP particle, the presence of subhalos can boost the signal since the annihilation rate is proportional to the square of the density. But while there is little doubt that dark matter halos are clumpy, the actual boost factor is a matter of some debate. In this paper, we take a critical look at the underlying assumptions in boost factor calculations and discuss the implications of our analysis for the ATIC and PAMELA results as well as current and future observations by the Fermi Gamma-Ray Large Area Space Telescope (GLAST) [4, 5, 6].

Halos in cosmological N-body simulations host numerous subhalos [7], which in turn host their own subhalos [8]. The distribution of subhalos can be summarized by the mass function, $dN/d\ln f$, where $f \equiv m/M_h$ is the relative mass fraction of a subhalo of mass m in a host of mass M_h . Note that in this paper, a host can refer to either a halo or a subhalo. The mass function appears to be well-characterized by a power-law [9, 10],

$$dN/d\ln f = Af^{-\alpha}, \quad (1)$$

for $f < 10^{-2}$. While current simulations probe $dN/d\ln f$ for $f \gtrsim 10^{-6}$, a Galactic-mass halo with neutralino dark matter should have subhalos down to $f \sim 10^{-18}$ [11], with the possibility of up to nine nested levels of substructure.

The luminosity of annihilation secondaries (electrons, positrons, or photons) from a halo or subhalo of mass M_h

can be written in the form

$$L_{e^\pm, \gamma} = \mathcal{P}_{e^\pm, \gamma} \frac{\langle \sigma v \rangle}{m_\chi} \mathcal{L}(M_h), \quad (2)$$

where $\mathcal{P}_{e^\pm, \gamma}$ are the branching ratios for electron-positron or photon secondaries, σ is the total annihilation cross section, and v and m_χ are the relative speed and mass of the annihilating particles. The quantity $\mathcal{L}(M_h)$ is the volume integral of ρ^2 where ρ is the dark matter density. The boost factor due to subhalos is defined implicitly by the relation

$$\mathcal{L}(M_h) = [1 + B(M_h)] \tilde{\mathcal{L}}(M_h). \quad (3)$$

Here $\tilde{\mathcal{L}}(M_h)$ represents the volume integral for a smooth halo, given by the volume integral of the smooth density field $\tilde{\rho}^2$. The boost factor is calculated recursively through the expression

$$B(M_h) = \frac{1}{\tilde{\mathcal{L}}(M_h)} \int \frac{dN}{d\ln f} [1 + B(m)] \tilde{\mathcal{L}}(m) d\ln f, \quad (4)$$

where $m = fM_h$.

Gamma-ray secondaries travel directly from the source to the observer and therefore the flux measured at Earth due to a source located at a distance d is $L_\gamma/4\pi d^2$. In contrast, charged particles are scattered by the Galactic magnetic field and therefore the arrival direction of the secondaries is essentially independent of the direction to the source. Furthermore, charged particles lose energy en route from the source to the observer. It is therefore useful to define an effective (energy-dependent) total boost due to all subhalos (see Ref. [12] for details):

$$B_{\text{eff}}(E; M_h, E_i, \mathbf{x}_\odot) = (1 - f_t)^2 + \frac{\mathcal{G}_{\text{sub}}(E; E_i, \mathbf{x}_\odot) \xi_{\text{sub}}(M_h)}{\xi_{\text{halo}}(E; E_i, \mathbf{x}_\odot)}. \quad (5)$$

Here f_t is the total mass fraction in subhalos and again $m = fM_h$. The first term accounts for the fact that $\tilde{\rho}$ is defined

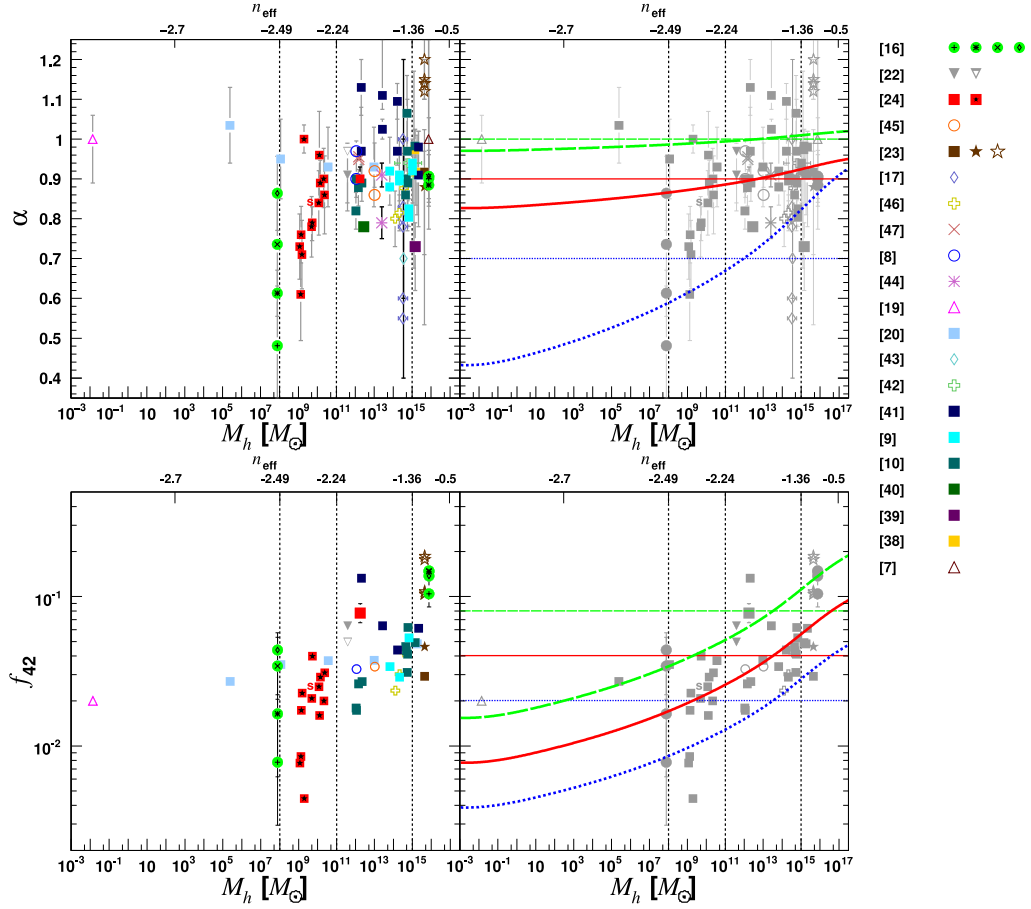


FIG. 1: Compilation of α (top) and f_{42} (bottom) from the studies indicated in right-hand key, where the year of the study decreases as one goes down the column. For both the upper and lower left panels, marker colors indicate different studies while the marker type indicate the algorithm used to identify subhalos. Studies which examined subhalo hosts instead of field halo hosts are indicated by internal black filled star. Colored horizontal error bars indicate mass range examined in study and black dashed vertical lines going from left to right indicate mass dwarf spheroidal galaxies, galaxies, and galaxy clusters. In the upper and lower right panels, we plot our phenomenological models of α and f_{42} with the thick and thin lines for model 1 and 0 respectively. For α , the mean, upper and lower values are given by the solid, dashed and dotted lines respectively. For f_{42} , the mean of the lognormal distribution is given by the solid line and $+2\sigma$ by the dashed, -2σ by the dotted lines. Top panels: vertical black and grey error bars indicate uncertainty in the published and fit-by-eye values respectively. Bottom panels: black vertical error bars indicate variation between similar mass hosts.

such that $\int \tilde{\rho} dV = M_h$, that is the halo is smooth, but only $(1 - f_t)$ of the host's mass is in the smooth radial component. Essentially $(1 - f_t)^2$ is a normalization term.

In Eq. (5), the effect of subhalos has been broken up into two terms by assuming that the volume distribution of subhalos is independent of mass distribution. The first term in the numerator, \mathcal{G}_{sub} , accounts for the propagation of cosmic rays originating from subhalos and is given by

$$\mathcal{G}_{\text{sub}}(E; E_i, \mathbf{x}_\odot) = \int G(E, \mathbf{x}_\odot; E_i, \mathbf{x}_i) \frac{\tilde{\rho}(\mathbf{x}_i)}{M_h} d^3 \mathbf{x}_i, \quad (6)$$

where the host term has been normalized by the solar density ρ_\odot . Here the propagation of the secondaries from an initial position \mathbf{x}_i with initial energy E_i to the Earth with final energy E is explicitly accounted for using the Green function $G(E, \mathbf{x}_\odot, E_i, \mathbf{x}_i)$. The propagation is a diffusive process and consequently $G(E, \mathbf{x}_\odot, E_i, \mathbf{x}_i) \propto \exp[-(\mathbf{x}_i - \mathbf{x}_\odot)^2 / \lambda_D^2(E; E_i)]$ where λ_D is the diffusion

length. For electron-positron pairs produced by a 100 – 1000 GeV WIMP, $\lambda_D \sim \text{few kpc}$ for $E \gtrsim 100$ GeV and decreases monotonically as $E \rightarrow E_i$ (see Ref. [12] for further discussion). In the definition of \mathcal{G}_{sub} , we are effectively treating subhalos as point sources, which is a reasonable assumption as $\approx 90\%$ of the flux originates from the central region of a (sub)halo. As we are interested in subhalos that are numerous enough to enhance the diffusive background, we are generally concerned with subhalos with masses of $\lesssim 10^8 M_\odot$. These halos have central regions that are $\lesssim \text{kpc}$ in radius. We also assume in Eq. (6) that subhalos trace the host's dark matter distribution.

The second term in the numerator, ξ_{sub} , is the total contribution of subhalos to the annihilation flux and is given by

$$\xi_{\text{sub}}(M_h) = \int \frac{dN}{d \ln f} \tilde{\mathcal{L}}(m) [1 + B(m)] d \ln f. \quad (7)$$

This is equivalent to the cosmic ray source term. The main

difference between our work and previous studies [12, 13, 14] is that we examine the enhancement that arises explicitly due to the entire subhalo hierarchy, that is subhalos, subsubhalos, etc., by incorporating the boost factor.

The ξ_{halo} term in denominator of Eq. (5) is the host's contribution to the cosmic ray flux which also accounts for the propagation of cosmic rays and is given by

$$\xi_{\text{halo}}(E; E_i, \mathbf{x}_\odot) = \int G(E, \mathbf{x}_\odot; E_i, \mathbf{x}_i) \tilde{\rho}^2(\mathbf{x}_i) d^3 \mathbf{x}_i, \quad (8)$$

Here again the propagation of the secondaries is explicitly accounted for using the Green function $G(E, \mathbf{x}_\odot, E_i, \mathbf{x}_i)$.

The effective boost in cosmic ray flux can be greatly enhanced by the boost factor. The boost factor depends sensitively on the subhalo mass function. Using the often quoted values $\alpha = 1$ and $A = 0.033$ [15], one finds $B \approx 30$ for γ -rays with a Galactic-mass halo. The key assumption in obtaining this result is that α and A are independent of the host mass and apply to all scales and levels in the subhalo hierarchy. Our goal is to examine the validity of this assumption, in short, to test whether α and A depend on the mass of the host. To do so, we compare estimates for α and A over a wide range of published simulations.

Though most of the results in our study are based on simulations which assume a standard Λ CDM cosmology, results from our own simulations of structure formation in scale-free cosmologies [16] as well as results from simulations of warm dark matter cosmologies [17] are also included. To assign an effective mass to hosts in these non-standard simulations we appeal to the halo formation process. In the hierarchical clustering paradigm, halos arise from primordial density fluctuations where small-scale structures form first and then merge together to form larger and larger objects. This process is governed by the power spectrum of the perturbations, $P(k)$, where k is the comoving wavenumber of a perturbation mode. Alternatively, one can describe the perturbation spectrum by the mass variance,

$$\sigma^2(M) = \int \frac{k^2 dk}{(2\pi)^3} P(k) W^2(k, M), \quad (9)$$

where $W(k, M)$ is the window function enclosing a mass $M \propto k^{-3}$ within a comoving volume of radius $r = 2\pi/k$. This quantity is simply the average rms overdensity of a sphere enclosing a mass M .

In scale-free cosmological models the primordial power spectrum is a power-law function of wavenumber k , that is, $P \propto k^n$ where n is referred to as the spectral index. This form of the power spectrum leads to a mass variance obeying $d \ln \sigma^2 / d \ln M = -(n + 3)/3$. Though the power-spectrum in a Λ CDM cosmology is more complicated, we can define an effective spectral index, $n_{\text{eff}}(M) \equiv -3(d \ln \sigma^2 / d \ln M + 1)$. Thus, the spectral index in a scale-free cosmology may be used as a proxy for the (Λ CDM) mass scale [16] by setting $n = n_{\text{eff}}(M)$ and solving for M . In this work we take $\Omega_m = 0.25$, $\Omega_\Lambda = 0.75$, $h = 0.73$, $\sigma_8 = 0.9$ and $n_s = 1$ as our reference cosmology.

The use of different algorithms to identify subhalos introduces a further complication. These algorithms range from

SUBFIND [18], which associates subhalos with local density peaks, to 6DFOF [16, 19], which searches for clustering in 6D phase space. In addition, some (but not all) researchers apply an unbinding criterion which removes unbound particles when estimating the mass of a subhalo. One reason for such a variety of methods is that subhalo identification is an ill-defined problem.

To characterize the amount of substructure, we introduce f_{42} in place of A , where

$$f_{42} = \int_{-4 \ln 10}^{-2 \ln 10} f \frac{dN}{d \ln f} d \ln f, \quad (10)$$

is the fraction of mass in subhalos with $10^{-2} < f < 10^{-4}$. In Fig. 1 we plot estimates of α and f_{42} from a large sample of studies. When available, we plot published values of α . Otherwise, we fit-by-eye for the mean α and estimate the uncertainty. The mean α is then used to determine f_{42} . Error bars for f_{42} are shown when a study reports the variation in the subhalo number or mass fraction across several hosts of the same mass.

The figure reveals a large amount of scatter in α and f_{42} . For galactic to cluster masses, estimates of α range from 0.7 and 1.1, which is generally within the estimated uncertainty in α for a single measurement and the variation in α with redshift for an individual halo [16, 20]. The scatter in $\log f_{42}$ is roughly constant with M_h with most points lying within 0.15 dex of the mean. The scatter may be due to variations in the mass accretion histories of the halos. The halo's mass accretion history is important not only for defining the density parameter [21] but it is also responsible for delivering new substructure within a halo.

Figure 1 also suggests that α and f_{42} decrease with decreasing M_h . The observed M_h -dependence should be treated with some caution. For example, a linear fit to $\alpha(M_h)$ for M_h between galaxy and cluster masses is consistent at the 1σ -level with $\alpha = \text{constant}$. Furthermore, at smaller host halo masses (n_{eff} closer to -3) the subhalo mass function is more sensitive to the type of subhalo-finding algorithm used [16] and in particular, whether a binding criterion is applied. For smaller M_h , subhalos tend to be less gravitationally bound. Studies that do not correct for unbound particles, such as [19], may overestimate subhalo masses and therefore overestimate α and f_{42} . Even for larger M_h , the application of a correction for unbound particles decreases α by 0.1 – 0.2 (see, for example, Ref. [22, 23]). It should also be noted that the data points from Ref. [24] at subgalactic masses are for subhalo hosts. This study found that the mass fraction of subsubhalos in subhalos tends to be smaller than the mass fraction of subhalos in halos. It may well be that α depends on the host's level in the subhalo hierarchy, that is α of a field halo may differ from that of a similar mass host that sits within the virial radius of a larger halo.

Most boost factor calculations assume α and f_{42} are independent of mass, that is, $\alpha(M_h) = \alpha_o$, $f_{42}(M_h) = f_o$. However, this assumption does not capture the trends in Fig. 1, especially at lower M_h , and we therefore propose the following

TABLE I: Summary of (α, f_{42}) model parameters

Model #	Fig. 2 color	α_o	α_n	f_o	f_n
0-u	g	1.0	0	0.04	0
0	r	0.9	0	0.04	0
0-l	b	0.7	0	0.04	0
1-u	g	1.0	0.046	0.034	10
1	r	0.9	0.12	0.034	10
1-l	b	0.7	0.46	0.034	10

phenomenological model:

$$\alpha(M_h) = \alpha_o + \alpha_n \log[n_{\text{eff}}(M_h) + 3], \quad (11)$$

$$\log f_{42}(M_h) = \log f_o + \log f_n \log[n_{\text{eff}}(M_h) + 3]. \quad (12)$$

We account for the scatter in α by considering three values for each α_o and α_n - the mean and the upper and lower envelop values as given in Table I. For f_{42} we fit the mean by eye and assume that it follows a lognormal distribution. This choice is motivated by the fact that other bulk halo parameters, such as the concentration parameter, follow lognormal distributions [25].

We calculate the boost factor using Eq. (4), under the assumption that the subhalo mass function is a power-law with an index $\alpha(M_h)$. The amplitude is normalized using $f_{42}(M_h)$ and $\alpha(M_h)$ subject to the condition that the total fraction of mass in subhalos is less than one. The mass function extends down to a mass m_o , the minimum CDM halo mass, which depends on the properties of the dark matter particle. Typical values for m_o when dark matter is a neutralino in the Constrained Minimal Supersymmetric Standard Model are $10^{-9} - 10^{-6} M_\odot$ [11], though the minimum CDM halo mass can vary between $10^{-12} - 10^{-4} M_\odot$ [26]. We use the more probable value of $m_o = 10^{-6} M_\odot$ [11]. We also assume that a host cannot contain subhalos with $f > 10^{-2}$ as suggested by most studies. As a consequence, the smallest host mass that contains subhalos is $100m_o$. Finally, we only go to three levels in the subhalo hierarchy since deeper levels change the boost factor by $\lesssim 1\%$. As a general observation the mass flux tends to come from the first two levels of the subhalo hierarchy.

Due to the condition that $f_t \leq 1$, the boost factors begin to saturate for large f_{42} and small m_o . The limiting values of f_{42} for a given α and m_o/M_h is given in Table II. This table shows that the limits are only important for $\alpha > 1$ and only when m_o/M_h is large, for example, when $m_o = 10^{-12} M_\odot$ for $M_h = 10^{12} M_\odot$. For our choice of $m_o = 10^{-6} M_\odot$, galactic mass hosts, and our subhalo mass function models, this saturation occurs at a f_{42} that is still $\approx 3\sigma$ away from the mean even at $\alpha = 1.0$.

The volume integral of $\tilde{\rho}^2$ in Eq. (3) is given by

$$\tilde{\mathcal{L}}(M_h) = \frac{\rho_v}{3} M_h c^3(M_h) g(c), \quad (13)$$

where ρ_v is the virial density of a halo, $c \equiv r_v/r_s$ is the concentration parameter, r_s is the profile's effective radius, and the dimensionless function $g(c)$ depends on the form of the

TABLE II: Limits on f_{42} due to $f_t \leq 1$

α	m_o/M_h	$f_{42,\text{lim}}$
0.8	10^{-24} to 10^{-16}	0.601 to 0.602
0.9	10^{-24} to 10^{-16}	0.371 to 0.384
1.0	10^{-24} to 10^{-16}	0.091 to 0.143

density profile. We consider the commonly used NFW [27] profile, which is described by two parameters, the characteristic radius r_s and density ρ_s . We also examine the Einasto profile, which appears to be a better fit to halos from cosmological simulations [24]. The Einasto profile has an extra parameter describing the radial logarithmic slope of the density profile which appears to have a mass dependence [28]. We find that an Einasto profile increases the boost factor for subgalactic masses by $\lesssim 50\%$. To determine the concentration parameter we use the two-parameter model presented in Ref. [25] for $c(M)$ as this model provides a better match to simulation data than the often-used model of Ref. [29]. Using the Ref. [25] model for $c(M)$ instead of the Ref. [29] model reduces B by $\lesssim 10\%$.

We calculate 10^4 random realizations of B for a given M_h where c and f_{42} are sampled from lognormal distributions with $\sigma_{\log f_{42}} = 0.15$ dex and $\sigma_{\log c} = 0.10$ dex [30]. Due to the recursive nature of Eq. (4), variation in c not only affects $\tilde{\mathcal{L}}$ of the host but that of the host's subhalos. The distribution of $B(M_h)$ across the 10^4 realizations appears to be well characterized by a lognormal distribution. We fit this distribution for the mean and the variance.

The results are plotted in Fig. 2. We particularly highlight the mass scales of the Galaxy's dwarf spheroidal satellites as these objects may be the best candidates for searches of γ -rays secondaries [5]. The left panel shows how a few key parameters individually affect $B(M_h)$. As a reference model, we use $m_o = 10^{-6} M_\odot$, $\alpha = 1.0$, $f_{42} = 0.067$, and an NFW density profile with the Bullock prescription for $c(M)$ [15]. Note that in Ref. [15], the boost factor is calculated for subhalos below the mass resolution of their *Via Lactea II* simulation, which is $\sim 10^5 M_\odot$. This amounts to calculating Eq. (4) with the upper limit given by $10^5 M_\odot/M_h$. Decreasing α from 1.0 to 0.9, or using the mean values from our new phenomenological model for f_{42} decreases $B(M_{\text{dSph}})$ by ~ 4 . The introduction of scatter in c and f_{42} increases the mean boost factor slightly, though the amount depends on the exact form and width of the distributions. For our choices, $B(M_{\text{dSph}})$ increases by $\approx 30\%$. Decreasing m_o to $10^{-9} M_\odot$ also increases the boost factor by $\approx 30\%$ while using an Einasto profile increases the boost factor by $\lesssim 20\%$ in this case.

The other two panels of Fig. 2 show the peak of the distribution and the 2σ contours from the models listed in Table I. We find increasing α increases the boost factor by ≈ 2 for dSph galaxies, though the differences are generally within the variation caused by c and f_{42} . For model 0, the mean α gives $B(M_{\text{dSph}}) \sim 0.6_{-0.4}^{+1.4}$, though for $\alpha = 1.0$, $B \sim 8$ is within the 2σ envelop. Model 1 reduces the boost factors such that $B(M_{\text{dSph}}) \gtrsim 2$ lie outside the 2σ envelop with the mean α giving $B(M_{\text{dSph}}) \approx 0.2$.

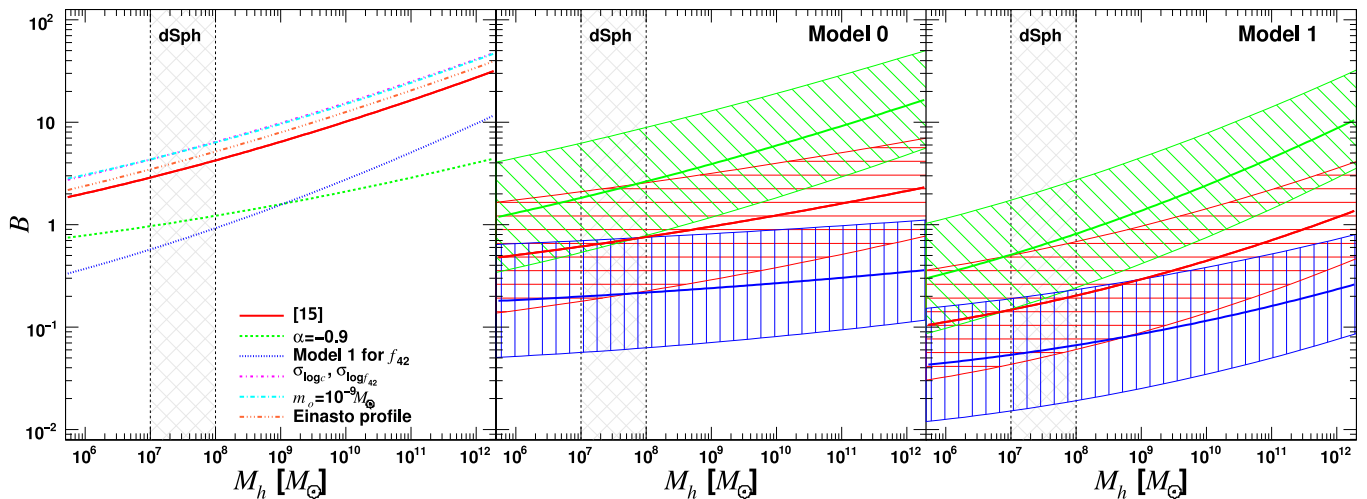


FIG. 2: Boost factors. Left panel shows how $B(M_h)$ changes when a single parameter is changed. Middle (right) panel shows model 0 (1) with thick red, green and blue lines indicating mean boost factor using the mean, upper, and lower values of α respectively. Colored hatched contours indicate the 2σ region arising from the variation in $\log c$ & $\log f_{42}$. The gray hatched region outlines the mass range for dwarf spheroidal satellite galaxies of MW.

Thus, subhalos in the Galaxy's satellites are unlikely to greatly enhance the γ -ray flux. Previous estimates of the number of satellites that could be detected via their γ -ray flux by GLAST, such as those by Ref. [5, 15], are probably overly optimistic. Even our revised calculations may overestimate the boost factor as it appears that subhalos have smaller f_{42} than similar mass halos. Consequently, satellites might even have their boost factors reduced by a factor of $\gtrsim 2$. So far, GLAST has detected numerous γ -ray sources, none of which are convincing dark matter annihilation signals [31].

We now examine the consequences of such boost factors for cosmic rays. To determine the energy dependence in Eq. (5), we use the mean propagation parameters listed in Ref. [12] and assume that the dark matter particle annihilates directly to monoenergetic e^\pm . For a 700 GeV thermal dark matter particle with $\langle\sigma v\rangle = 3 \times 10^{-26} \text{ cm}^3 \text{ s}^{-1}$, the diffusion length is 1.3 kpc at $E = 300$ GeV and monotonically decreases to 0.1 kpc at $E = 690$ GeV. We also assume that the Milky Way halo has an NFW density profile with a characteristic radius $r_s = 20$ kpc and a solar density of $\rho_\odot = 0.43 \text{ GeV cm}^{-3}$.

Recall that in Eq. (5) we assumed that the subhalo volume distribution is the same as the halo's density profile. However, simulations appear to show that subhalos do not trace the host halo's radial density profile [24, 35]. Instead tidal stripping destroys subhalos in the center, resulting in a radially anti-biased distribution, at least for subhalos with masses of $\gtrsim 10^5 M_\odot$. Very few subhalos are thus found within ~ 20 kpc of the halo center. This implies is that subhalos are unlikely to contribute to the observed flux as they are too far away. We argue that it is unreasonable to assume that this anti-biased radial distribution continues down to very small masses since these subhalos should become increasingly less susceptible to tidal disruption as their mass decreases and therefore should be able to survive to smaller radii. It is also worth noting that it is difficult to identify substructure in the central, high

density regions of halos with current group finder algorithms. Furthermore, Ref. [35] found that though tidal fields affect the mass of subhalos, their annihilation luminosity is less affected and more closely follows the host halo's radial density profile. Thus, we compromise and only include contributions from subhalos with $m \lesssim 10^4 M_\odot$. Considering only low mass subhalo hosts reduces the contribution of substructure by $\approx 60\%$ for both models 0 and 1. This may still be an optimistic assumption since interactions with baryonic matter, that is the Galactic disk and stars, might further reduce the inner subhalo abundance.

In general we find $B_{\text{eff}}(E \geq 300 \text{ GeV}) \sim 1$. Even the most optimistic model, 0-u, gives $B_{\text{eff}}(E \geq 300 \text{ GeV}) = 1.3_{-0.4}^{+0.6}$. Here the variation in B_{eff} is due primarily to the variation in f_{42} for the Galactic halo based on our phenomenological model, though we also account for the variation in the boost factors and concentration parameters of subhalos. This model excludes the $B_{\text{eff}} \sim 200$ required to explain the ATIC signal at the $\sim 14\sigma$ level. These results are in agreement with similar studies [12, 13, 14]. We have improved on earlier results by explicitly including several levels in the subhalo hierarchy that earlier work neglected.

The High Energy Stereoscopic System (HESS) [34] and Fermi GLAST [4] found different though not necessarily contradictory results. Both instruments detect an excess, though not as large as that observed by ATIC, and neither instrument observes the pronounced peak at ~ 700 GeV seen by ATIC. The Fermi GLAST measurements require a boost of ~ 150 at $E = 300$ which monotonically decreases to ≈ 70 at $E = 600$. This is still rejected by our model at the $10 - 12\sigma$ level.

Some studies have suggested that it is possible to reproduce the observed flux, particularly the ATIC bump in the energy spectrum, with a single nearby subhalo [14, 32]. The required annihilation rate is $\sim 10^{37} \text{ s}^{-1}$ for a thermal WIMP with $m_\chi \sim 100 - 1000 \text{ GeV}$. Neglecting the boost factor from

deeper levels in the subhalo hierarchy, a subhalo with a mass of $\gtrsim 10^8 M_\odot$ at ~ 1 kpc is required. However, Ref. [33] find based on a numerical simulation that the probability of such a large subhalo within ~ 8 kpc of the Galactic center is exceedingly low, $p \lesssim 10^{-5}$. This clearly appears to be highly unlikely. Incorporating the boost factors, and thereby incorporating the entire subhalo hierarchy, does not drastically reduce the minimum mass required to explain the ATIC peak and thereby the probability of a nearby clump.

The anomalous cosmic ray flux observed by ATIC and PAMELA have sparked a flurry of interest as there is the possibility that these instruments may have indirectly detected annihilating dark matter. However, the observed amplitude cannot be explained with standard thermal dark matter. A number of studies have invoked subhalos to explain the large amplitude of this flux. Our work effectively ends this line of thought.

We find that subhalos alone are unlikely to account for the anomaly and are strongly ruled out at the 14σ level. This still leaves the possibility that the flux is due to instrument errors, astrophysical phenomena, or, more intriguingly, perhaps exotic theories of dark matter are required [36, 37].

Acknowledgments

The authors thank the anonymous referees for useful comments. PJE acknowledges funding from the NSERC. RJT and LMW acknowledge funding by respective Discovery Grants from NSERC. RJT is also supported by grants from the Canada Foundation for Innovation and the Canada Research Chairs Program.

-
- [1] J. Chang, et al., *Nature* **456**, 362 (2008).
 - [2] O. Adriani, et al., *Nature* **458**, 607 (2009).
 - [3] G. Bertone, D. Hooper, and J. Silk, *Phys. Rep.* **405**, 279 (2005).
 - [4] A. A. Abdo, et al., *Physical Review Letters* **102**, 181101 (2009).
 - [5] L. E. Strigari, S. M. Koushiappas, J. S. Bullock, and M. Kaplinghat, *Phys. Rev. D* **75**, 083526 (2007).
 - [6] L. Pieri, G. Bertone, and E. Branchini, *MNRAS* **384**, 1627 (2008).
 - [7] B. Moore, et al., *ApJ* **524**, L19 (1999).
 - [8] J. Diemand, M. Kuhlen, and P. Madau, *ApJ* **657**, 262 (2007).
 - [9] L. Gao, et al., *MNRAS* **355**, 819 (2004).
 - [10] J. Diemand, B. Moore, and J. Stadel, *MNRAS* **352**, 535 (2004).
 - [11] G. D. Martinez, et al., *ArXiv e-prints* (2009), 0902.4715.
 - [12] J. Lavalle, et al., *A&A* **479**, 427 (2008).
 - [13] M. Pato, L. Pieri, and G. Bertone, *ArXiv e-prints* (2009), 0905.0372.
 - [14] M. Kuhlen and D. Malyshev, *Phys. Rev. D* **79**, 123517 (2009).
 - [15] M. Kuhlen, J. Diemand, and P. Madau, *ApJ* **686**, 262 (2008).
 - [16] P. J. Elahi, et al., *MNRAS* **395**, 1950 (2009).
 - [17] A. Knebe, et al., *MNRAS* **386**, 1029 (2008).
 - [18] V. Springel, et al., *MNRAS* **328**, 726 (2001).
 - [19] J. Diemand, M. Kuhlen, and P. Madau, *ApJ* **649**, 1 (2006).
 - [20] L. Gao, et al., *MNRAS* **363**, 379 (2005).
 - [21] A. Tasitsiomi, et al., *ApJ* **607**, 125 (2004).
 - [22] E. Athanassoula, et al., *Astroparticle Physics* **31**, 37 (2009).
 - [23] M. Maciejewski, et al., F. R. Bouchet, *MNRAS* **396**, 1329 (2009).
 - [24] V. Springel, et al., *MNRAS* **391**, 1685 (2008).
 - [25] A. V. Macciò, A. A. Dutton, and F. C. van den Bosch, *MNRAS* **391**, 1940 (2008).
 - [26] S. Profumo, K. Sigurdson, and M. Kamionkowski, *Physical Review Letters* **97**, 031301 (2006).
 - [27] J. F. Navarro, C. S. Frenk, and S. D. M. White, *ApJ* **490**, 493 (1997).
 - [28] L. Gao, et al., *MNRAS* **387**, 536 (2008).
 - [29] J. S. Bullock, et al., *MNRAS* **321**, 559 (2001).
 - [30] A. F. Neto, et al., *MNRAS* **381**, 1450 (2007).
 - [31] A. A. Abdo, *ArXiv e-prints* (2009), 0902.1340.
 - [32] D. Hooper, A. Stebbins, and K. M. Zurek, *Phys. Rev. D* **79**, 103513 (2009).
 - [33] P. Brun, et al., *ArXiv e-prints* (2009), 0904.0812.
 - [34] H. E. S. S. Collaboration: F. Aharonian, *ArXiv e-prints* (2009), 0905.0105.
 - [35] J. Diemand and B. Moore, *ArXiv e-prints* (2009), 0906.4340.
 - [36] N. Arkani-Hamed, D. P. Finkbeiner, T. R. Slatyer, and N. Weiner, *Phys. Rev. D* **79**, 015014 (2009).
 - [37] M. Kuhlen, P. Madau, and J. Silk, *ArXiv e-prints* (2009), 0907.0005.
 - [38] S. Ghigna, et al., *ApJ* **544**, 616 (2000).
 - [39] A. Helmi, S. D. M. White, and V. Springel, *Phys. Rev. D* **66**, 063502 (2002).
 - [40] F. Stoehr, et al., *MNRAS* **345**, 1313 (2003).
 - [41] G. De Lucia, et al., *MNRAS* **348**, 333 (2004).
 - [42] F. C. van den Bosch, G. Tormen, and C. Giocoli, *MNRAS* **359**, 1029 (2005).
 - [43] S. P. D. Gill, A. Knebe, and B. K. Gibson, *MNRAS* **356**, 1327 (2005).
 - [44] L. D. Shaw, et al., *ApJ* **659**, 1082 (2007).
 - [45] P. Madau, J. Diemand, and M. Kuhlen, *ApJ* **679**, 1260 (2008).
 - [46] C. Giocoli, G. Tormen, and F. C. van den Bosch, *MNRAS* **386**, 2135 (2008).
 - [47] C. Giocoli, L. Pieri, and G. Tormen, *MNRAS* **387**, 689 (2008).